RadioGraphics

Thoracic Paracoccidioidomycosis: Radiographic and CT Findings[1]

Miriam M. Barreto, MD, PhD • Edson Marchiori, MD, PhD • Viviane B. Amorim, MD • Gláucia Zanetti, MD • Tatiana C. Takayassu, MD • Dante L. Escuissato, MD, PhD • Arthur S. Souza, Jr, MD, PhD • Rosana S. Rodrigues, MD, PhD

ONLINE-ONLY CME

See www.rsna.org/education/rg_cme.html

LEARNING OBJECTIVES

After completing this journal-based CME activity, participants will be able to:

- Describe the abnormalities most commonly seen at imaging of PCM.
- List the most important clinical and epidemiologic features of PCM.
- Discuss the correlation of radiologic and histologic findings of PCM.

TEACHING POINTS

See last page

Paracoccidioidomycosis (PCM) is the most common systemic mycosis in Latin America. Although most cases occur in developing countries, recent immigration patterns and an increase in travel have led to a growing number of PCM cases in the United States and Europe. PCM is caused by the dimorphic fungus *Paracoccidioides brasiliensis*, and the chronic form may progress to severe pulmonary involvement. Several radiologic patterns have been described for pulmonary PCM, including linear and reticular opacities, variable-sized nodules, patchy ill-defined opacities, airspace consolidation, and cavitary lesions. Fibrosis and paracicatricial emphysema are common associated findings. Chest computed tomography (CT) is the method of choice for evaluating pulmonary PCM, with the most common CT findings being ground-glass attenuation, consolidation, small or large nodules, masses, cavitations, interlobular septal thickening, emphysema, and fibrotic lesions. PCM is also an important cause of the "reversed halo" sign at high-resolution CT and should be considered in the differential diagnosis. Awareness of the multiple radiologic manifestations of PCM as well as its epidemiologic and clinical characteristics may permit early diagnosis and initiation of specific treatment, thereby reducing associated morbidity and mortality.

Abbreviations: AIDS = acquired immunodeficiency syndrome, PCM = paracoccidioidomycosis

RadioGraphics 2012; 32:71–84 • **Published online** 10.1148/rg.321115052 • **Content Codes:** CH CT

[1]From the Department of Radiology, Federal University of Rio de Janeiro, Rúa Thomaz Cameron 438, Valparaiso CEP 25685.120, Petrópolis, Rio de Janeiro, Brazil (M.M.B., E.M., V.B.A., G.Z., T.C.T., R.S.R.); Department of Radiology, Federal University of Paraná, Curitiba, Brazil (D.L.E.); Faculty of Medicine, São José do Rio Preto, São José do Rio Preto, Brazil (A.S.S.); and D'Or Institute for Research and Education, Rio de Janeiro, Brazil (R.S.R.). Recipient of a Certificate of Merit award for an education exhibit at the 2010 RSNA Annual Meeting. Received March 15, 2011; revision requested May 6 and received June 5; accepted June 24. For this journal-based CME activity, the authors, editor, and reviewers have no relevant relationships to disclose. **Address correspondence to** E.M. (e-mail: *edmarchiori@bol.com.br*).

Introduction

Paracoccidioidomycosis (PCM) is becoming relevant worldwide, with increasing numbers of cases having been detected among immigrants and in travelers returning from regions where PCM is endemic (1–3). PCM is caused by *Paracoccidioides brasiliensis*, a thermally dimorphic fungus that grows as a budding yeast in host tissue and as a yeast or mold in culture medium at 37°C. The disease is acquired by inhalation of infectious particles that reach the lungs and cause the primary infection (4–6). PCM is characterized by pulmonary involvement, lymphadenopathy, and chronic progression of mucocutaneous lesions.

Teaching Point

The lungs are the main target organ of *P brasiliensis*, and chronic changes are responsible for the morbidity and mortality associated with PCM (5). Active pulmonary involvement has been reported in 80% of PCM cases and residual fibrotic lesions in 60% (7).

In this article, we discuss PCM in terms of its causal organism, epidemiologic features, pathogenesis, clinical course, diagnosis, and histologic findings. In addition, we describe the radiographic and computed tomographic (CT) manifestations of thoracic involvement, as well as pulmonary and extrapulmonary abnormalities.

Causal Organism

P brasiliensis colonies are composed of yeast cells of different sizes (4–30 μm), usually with an oval or elongated shape, with multiple budding cells having a thick, well-defined refractile cell wall (Fig 1). The mycelial form grows after 20–30 days of incubation at room temperature (8,9).

Teaching Point

The diagnosis of PCM is established with visualization of *P brasiliensis*, either at direct examination or after isolation of the fungus at culture, in biologic specimens such as sputum, bronchoalveolar lavage fluid, smears from mucocutaneous lesions, or tissue biopsy samples from laryngeal lesions, cervical lymph nodes, or lung (10). Staining with methenamine–silver nitrate (Grocott-Gomori) stain is the main method for visualizing typical fungal elements of *P brasiliensis*, such as the yeastlike multiple budding that mimics a pilot's wheel (8). Serologic tests such as immunodiffusion generally provide results earlier than does histologic analysis and can be helpful in making the diagnosis (11,12).

Epidemiologic Features

PCM, formerly known as South American blastomycosis, is the most common systemic mycosis in Latin America. An estimated 10 million people in this endemic area have been affected (8,13). Almost all South and Central American countries have large regions where PCM is endemic, particularly Brazil, Colombia, Venezuela, and Argentina (11). However, several cases of PCM have been reported in Europe and North America, mainly among immigrants and in travelers who had left the endemic area 3–20 years earlier (2,14,15).

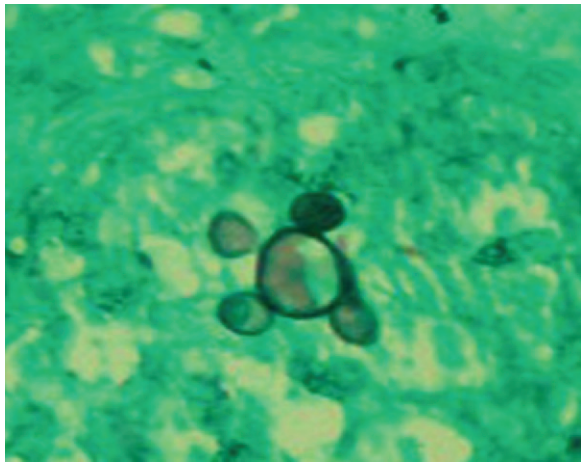

Figure 1. Photomicrograph (original magnification, ×100; Grocott-Gomori methenamine–silver nitrate stain) shows the typical round form of *P brasiliensis* with budding, findings that resemble a pilot's wheel.

The most severely endemic areas of PCM worldwide are the subtropical regions of Brazil, where PCM is estimated to affect up to 10% of the population, being particularly prevalent among farm workers. The disease predominantly affects men between 30 and 60 years of age from rural areas because of their exposure to the fungus habitat (soil) (11,16,17). The average male-to-female ratio of infection is 13:1 in South American countries (17).

Pathogenesis

Like tuberculosis and histoplasmosis, PCM is most commonly acquired through the inhalation of infective particles, which cause a self-limited, inflammatory parenchymal lung infection (5,18). The initial lesion is similar to the primary complex of tuberculosis and may be controlled by natural defense mechanisms or may progress to symptomatic disease. The fungus can then spread by lymphatic or blood circulation to the kidneys, spleen, liver, bone, adrenal glands, central nervous system, and airways, including the trachea (11,14,19,20). Oral lesions are present in over 50% of cases and usually occur through contamination of the oral mucosa by eliminated lung secretions. In most cases, the skin is affected by hematogenous dissemination. Although rare, skin

inoculation may also occur if a traumatic lesion comes into contact with vegetable matter or contaminated soil materials (21–23).

Although neutrophils participate in the early inflammatory response to *P brasiliensis*, the predominant tissue reaction is granulomatous. In an immunocompetent host, cellular immunity is the key defense mechanism against fungal infection (8,9).

The lung is the most commonly affected organ (50%–100% of cases) and is the site of lesions associated with both the acute and chronic forms of infection (7,18,24). Once *P brasiliensis* infectious propagules reach the lungs and convert into the yeast form in a susceptible host, dissemination throughout the pulmonary structures occurs, frequently producing extensive local damage that later results in respiratory failure (5,7,14).

Clinical Course

Teaching Point

Clinical forms of PCM range from a benign self-limited infection to a severe, progressive, and sometimes fatal disease involving pulmonary and extrapulmonary tissues. The two main clinical forms of PCM are the acute form (juvenile type) and the chronic form (adult type). The chronic form of the disease may develop many years after patients have left an endemic area (3,4,11,12,25,26).

The acute form of PCM represents 3%–5% of all cases and affects children, adolescents, and young adults. It is characterized by marked involvement of the reticuloendothelial system (spleen, liver, lymph nodes), the gastrointestinal tract, and, rarely, the bones. Although *P brasiliensis* enters through the lung, pulmonary involvement by acute PCM is rarely detected clinically or radiologically. The acute form develops within weeks or months and is more severe than the chronic form, leading to significantly higher rates of mortality (1,11,12,26,27).

The chronic form, which accounts for 90% of cases, results from reactivation of quiescent lung lesions. It mainly affects men over 30 years of age and has an insidious course. The lungs are the most frequently involved organ, leading to significant morbidity due to impairment of lung function (5,7). Patients with chronic PCM may be asymptomatic initially but may go on to experience severe pulmonary involvement with intense coughing and shortness of breath. Pulmonary symptoms are nonspecific and include chronic cough, expectoration, dyspnea, chest pain, and hemoptysis, with or without systemic manifestations such as weight loss, fever, or anorexia (6,28).

In chronic PCM, the lungs are affected in more than 90% of cases, either in isolation or in association with other organs (especially the skin, mucous membranes, adrenal glands, bones, and central nervous system). Isolated lesions in these organs occur without lung involvement in about 10% of cases (5,11,21,29).

Mucous membranes are rarely involved in acute PCM, although cutaneous compromise is common (54% of cases). In contrast, oropharyngeal mucous membrane lesions occur in about 50% of chronic cases, and isolated cutaneous lesions are uncommon. About 50% of patients who present with pulmonary lesions do not develop mucosal lesions (21–23,29–31).

The silent course of PCM and the dissociation between clinical and radiologic findings often result in the steady progression of lung damage. Patients from PCM-endemic areas with chronic, nonspecific constitutional symptoms should be examined radiologically. PCM should be diagnosed on the basis of findings at pulmonary CT, and therapy can be initiated after the diagnosis is confirmed. Treatment has profoundly changed the outcome of patients with PCM and is essential for avoiding progression of fungal disease and death. Early diagnosis should be made, and prompt initiation of treatment is necessary to avoid the development of fibrosis but does not appear to modify the fibrotic sequelae of the lungs (7,17).

P brasiliensis infection is relatively rare in immunocompromised patients, including patients with acquired immunodeficiency syndrome (AIDS), transplant recipients, or patients with hematologic malignancies. In AIDS patients, PCM most frequently manifests as disseminated disease with prolonged fever, weight loss, lymphadenopathy, splenomegaly, hepatomegaly, and skin rash (8). It may mimic other diseases, which often leads to erroneous or delayed treatment. Of note, AIDS is a predominantly urban disease, in contrast to the rural prevalence of PCM (32,33).

Diagnosis

Healthy subjects living in endemic areas may be infected by inhalation of the infective forms of *P brasiliensis* and are usually asymptomatic but can develop either acute PCM, with severe involvement of internal organs and the mononuclear phagocyte system, or chronic PCM, with an insidious evolution and involvement of the lungs and mucosa (11,12).

In patients with chronic PCM, respiratory symptoms can be scarce, indicating a clinical-radiologic dissociation. Associated lesions of the oral mucosa, tongue, palate, pharynx, and vocal

cords predominate. Lymphadenopathy involving mainly the cervical chains is also common (5,11). Acute PCM affects children, adolescents, and young adults (as mentioned earlier) of both sexes and is more severe, with a rapid course. Affected patients usually present with hepatosplenomegaly, lymphadenopathy, or, rarely, osteoarticular lesions (1,11,12,26,27).

Definitive diagnosis should be based on the detection of fungal elements at microscopic examination of fresh clinical specimens (sputum, mucocutaneous lesions, ganglionary aspirate) or biopsy material (skin, mucosae, lymph nodes). This can be complemented by culture and isolation of the fungus in modified Sabouraud medium (12,20). The standard of reference for the diagnosis of PCM is direct visualization of the typical budding yeast structures of *P brasiliensis*, properly stained with Grocott-Gomori methenamine–silver nitrate or periodic acid–Schiff stain (1,8,11).

Specific serologic tests generally provide results faster than does culture and are important both as a diagnostic tool and for assessing treatment response (1,11). If standard techniques and appropriate antigens are used, these tests can have a sensitivity and specificity of 85%–100%. However, lack of a serologic response does not exclude PCM, particularly in immunocompromised patients, including those with human immunodeficiency virus–AIDS (8,11,20).

Histologic Findings

Histologic findings can be classified into three basic patterns—pneumonic, granulomatous, and fibrotic—that correlate with the patterns seen at high-resolution CT (34). The pneumonic form is characterized by acute alveolitis, in which the fungus is found within histiocytes or extracellularly (34). Early lesions occur in the alveolar tissue, with a nonspecific mononuclear inflammatory or granulomatous interstitial infiltrate in the alveolar septa, and have a tendency toward cicatricial organization. For intraalveolar injuries, two main types have been described: exudative and productive granulomatous (35). The extreme form of the exudative type is a purulent inflammation that destroys the lung tissue, eventually leading to abscess formation (35,36).

The granulomatous form is characterized by circumscribed epithelioid granulomas in the pulmonary interstitium, typically with few organisms engulfed by giant cells and monocytes from the granulomatous reaction. A proliferation of reticulin fibers is seen, especially at the periphery of the granulomas, connecting these structures and spreading to adjacent alveolar walls (34). This pattern, also known as the nodular form, can manifest as miliary nodules or acinar nodules. Acinar nodules may coalesce, resembling findings of lung consolidation and bronchopneumonia. The nodules may become necrotic, resulting in abscesses and cavities (35,37). Miliary nodules can be seen in other organs, presumably due to hematogenous dissemination, resembling tuberculosis (36).

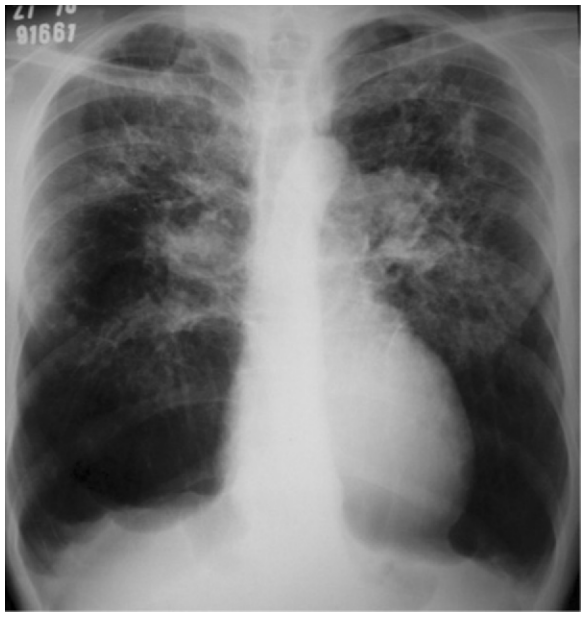

Figure 2. Chronic pulmonary PCM in a 65-year-old man. Chest radiograph demonstrates bilateral reticular opacities, more prominent in the central areas ("butterfly wing" pattern), with associated parenchymal distortion and lower lobe emphysema.

The fibrotic form is characterized by thickening of the interlobular and alveolar septa due to the proliferation of collagen fibers (34). Pulmonary fibrosis can be a prominent finding in both the granulomatous and pneumonic forms (36). The extent of fibrotic phenomena in the lungs is associated with either the introduction of specific therapy or the typically slow chronic progression of the disease (35). Large areas of fibrosis occur, especially close to the hilar region, enveloping lymph nodes, the main bronchi, and branches of the pulmonary artery. Hilar fibrosis follows the pulmonary lymphatic distribution, probably resulting from previous specific lymphangitic spread of PCM (10,34). Paracicatricial emphysema, either bullous or panacinar type, is a common finding. Rupture of the bullae may cause spontaneous pneumothorax (37).

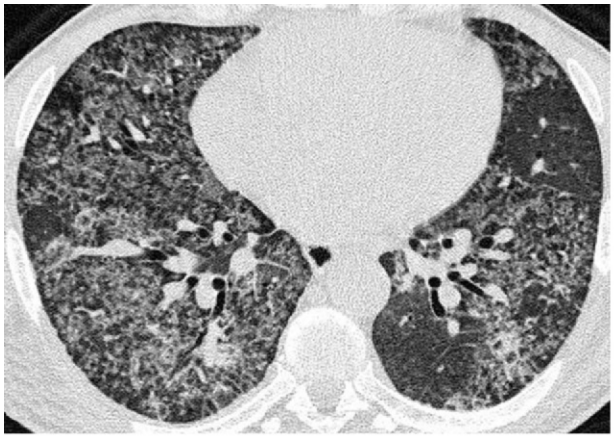

3.

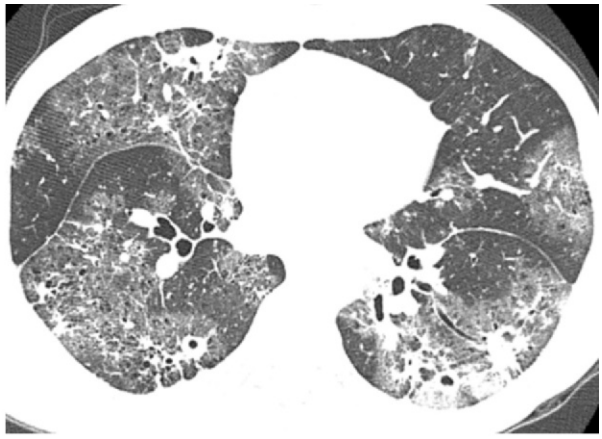

4.

Figures 3, 4. **(3)** Chronic pulmonary PCM in a 58-year-old man. High-resolution CT scan at the level of the lower lobes depicts patchy ground-glass attenuation. **(4)** Chronic pulmonary PCM in a 50-year-old man. High-resolution CT scan shows diffusely distributed ground-glass attenuation and cavitated nodules in both lungs, with associated mild parenchymal distortion.

Radiologic Manifestations of Pulmonary Infection

Chest Radiography

Many different reports have described the polymorphic chest radiographic patterns of chronic pulmonary PCM, including alveolar, interstitial, and mixed patterns, usually bilateral and involving more than one-third of the lungs (18,38). Recognizing the large variety of pulmonary radiographic alterations that can occur is essential.

Although a pulmonary cycle occurs in the acute form of PCM, with an initial lesion resembling the primary complex of tuberculosis, these findings are rarely demonstrated radiologically. Isolated hilar enlargement has occasionally been seen on chest radiographs obtained in patients with acute PCM. However, the evolution of the acute form of PCM from a primary lung–lymph node complex to a severe disseminated disease that rarely affects the lungs remains poorly understood (4).

Teaching Point

Chest radiographic lung abnormalities in chronic PCM are frequently multiple and nonspecific (7,38). They have been variously described as linear reticular opacities, nodules of various sizes, patchy ill-defined opacities, airspace consolidation, and cavitation (5,6,10,15,17,18,38). In endemic areas, bilateral and symmetric opacities in the middle zones of the lungs with associated emphysema in the lung bases should suggest the disease (Fig 2). This finding is also known as the butterfly wing pattern (18).

In chronic pulmonary PCM, architectural distortion, paracicatricial emphysema, and traction bronchiectasis are common manifestations of pulmonary fibrosis (5,7).

Lymphadenopathy and pleural effusions, when present, are frequently associated with the acute form of PCM (1,4). Mediastinal and hilar lymphadenopathy, pleural effusions, and pulmonary calcifications occur only rarely in the chronic form (5,18,24).

Computed Tomography

CT is more sensitive than chest radiography in assessing the pattern and distribution of parenchymal abnormalities. The most common CT findings of chronic PCM are ground-glass areas of enhancement, consolidations, variable-sized nodules, masses, cavitations, interlobular septal thickening, and fibrotic lesions (5,17). A combination of these findings is observed in most cases and may be focal, multifocal, or diffuse. The disease distribution is usually bilateral and symmetric, with involvement predominantly of the peripheral and posterior regions. All lung zones are affected, with a discrete predominance in the middle zones (5,10,17). Extrapulmonary abnormalities can also occur.

Teaching Point

Pulmonary Abnormalities

Ground-Glass Attenuation

Ground-glass attenuation is the most common high-resolution CT finding in patients who have not yet been treated for PCM infection (17). It is commonly patchy without a specific distribution (Figs 3, 4). In most cases, the ground-glass pattern reflects the presence of alveolar septal thickening due to inflammation, with or without

Figures 5–8. **(5)** Chronic pulmonary PCM in a 47-year-old woman. CT scan demonstrates multifocal peripheral consolidations with traction bronchiectasis in the middle and lower lobes. **(6)** Chronic pulmonary PCM in a 42-year-old man. High-resolution CT scan shows bilateral consolidations with associated multiple confluent small nodules and interlobular septal thickening, more prominent in the central lung zones. **(7)** Chronic PCM in a 49-year-old man. High-resolution CT scan shows irregular airspace consolidations with associated cavitation, traction bronchiectasis, and architectural distortion, mainly in the right upper lobe. Ground-glass attenuation and small nodular areas of enhancement are also seen. **(8)** Chronic PCM in a 37-year-old man. High-resolution CT scan shows extensive consolidation in both upper lobes, with associated architectural distortion and areas of cavitation.

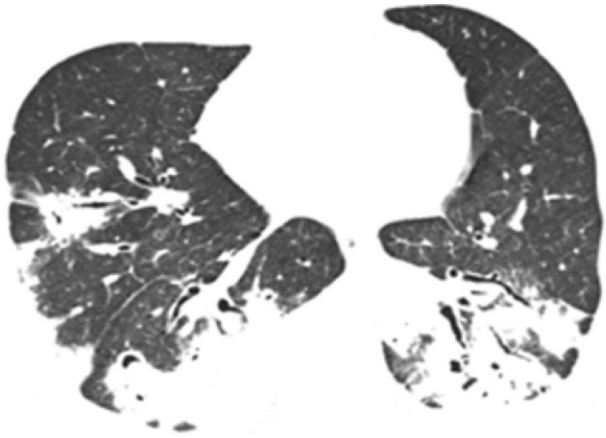

5.

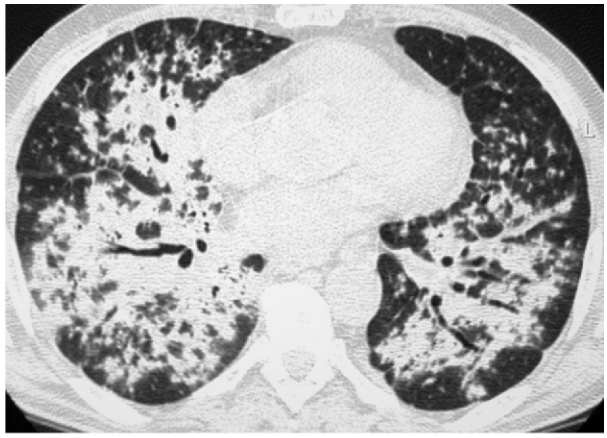

6.

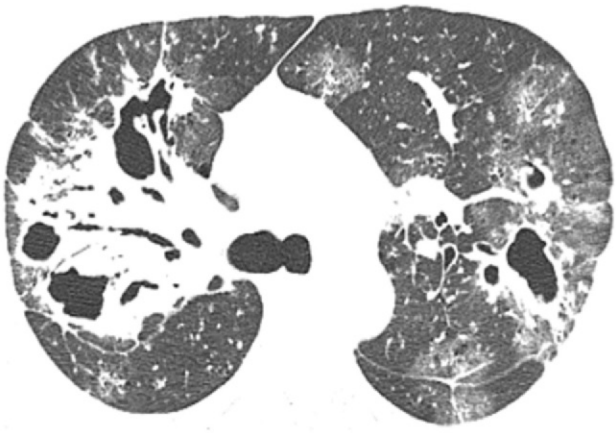

7.

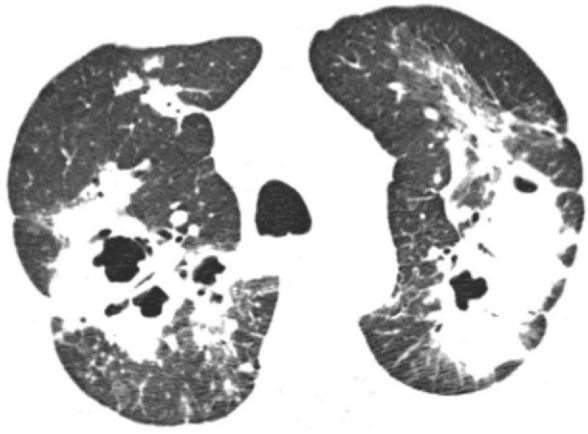

8.

airspace filling. Ground-glass attenuation may also result from fibrosis of the alveolar septa, with associated architectural distortion and a honeycomb pattern (10).

Consolidation

Airspace consolidation results from filling of the alveoli by an acute inflammatory exudate where the fungus is abundant (Figs 5, 6). This pattern is described in the literature as the pneumonic form. Fibrosis, necrosis, and cavitation frequently occur with progression of the disease (Figs 7, 8) (5,10).

Nodular Pattern

Nodules of various sizes are commonly seen, resulting from inflammatory exudates filling alveolar spaces. The nodular pattern can be miliary (Fig 9) or macronodular (Fig 10). The macronodules may be rounded or lobulated and either isolated or confluent, similar to pneumonic or bronchopneumonic consolidations (5). The nodules may also have ground-glass attenuation (Fig 11) or manifest with necrosis and cavitation (Fig 12).

The small random nodules (Fig 9) in patients with PCM frequently have irregular shapes, reflecting confluent granulomas. This pattern is described in the literature as the granulomatous form, which is characterized by epithelioid granulomas in the pulmonary interstitium, typically with few engulfed organisms (10).

Figures 9–12. **(9)** Chronic pulmonary PCM in a 39-year-old man. High-resolution CT scans of the upper **(a)** and lower **(b)** lobes depict multiple pulmonary micronodules in a random distribution consistent with a miliary pattern. **(10)** Chronic pulmonary PCM in a 39-year-old woman. High-resolution CT scan shows several large, irregular nodules in both lungs. Discrete ground-glass attenuation and small nodular areas of enhancement are seen around some of the nodules. **(11)** Chronic pulmonary PCM in a 48-year-old man. CT scan demonstrates several variable-sized nodules with ground-glass attenuation in both lungs (arrows), predominantly on the right side, as well as a left perihilar irregular cavitated consolidation. **(12)** Chronic pulmonary PCM in a 44-year-old man. CT scan depicts multiple variable-sized cavitary nodules in both lungs. Note also the bronchial wall thickening (arrows) on the right side.

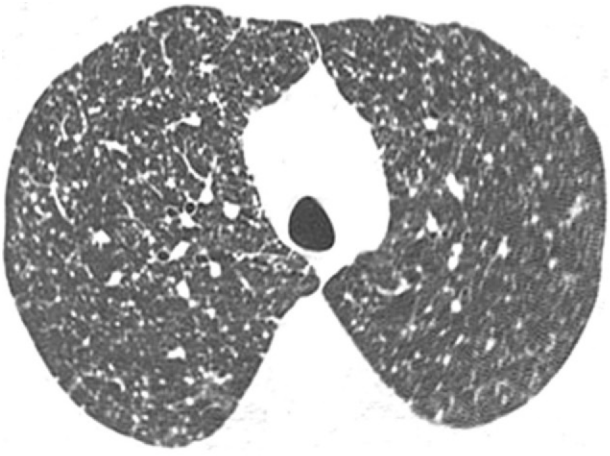

9a.

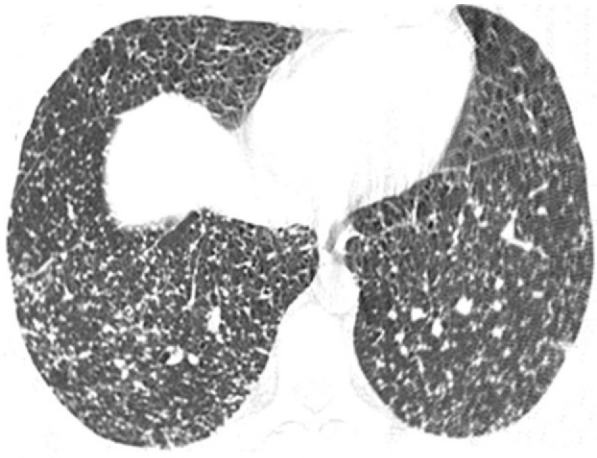

9b.

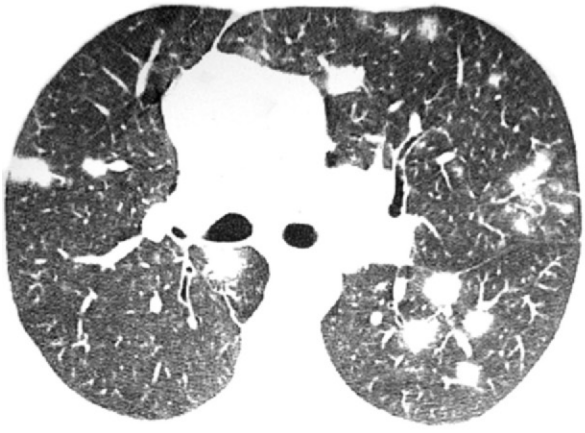

10.

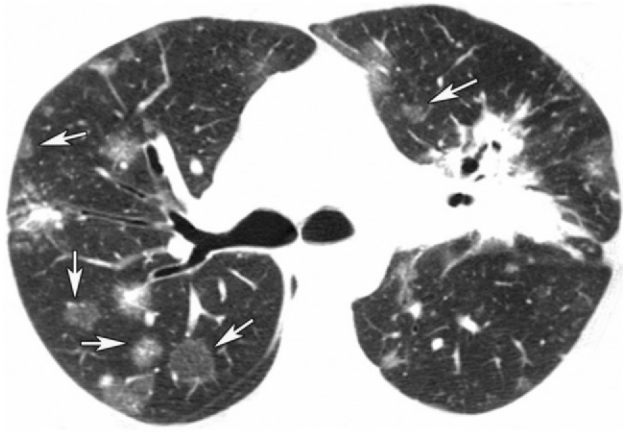

11.

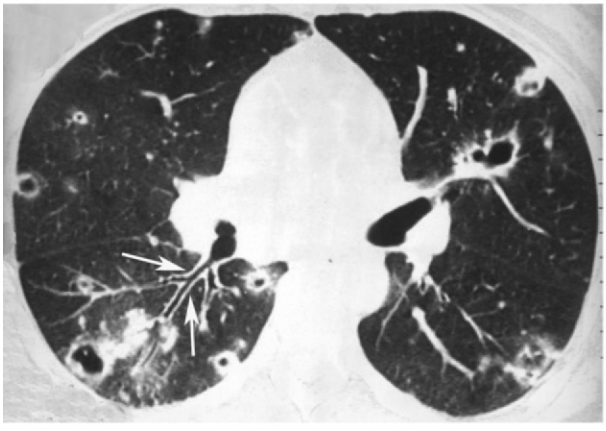

12.

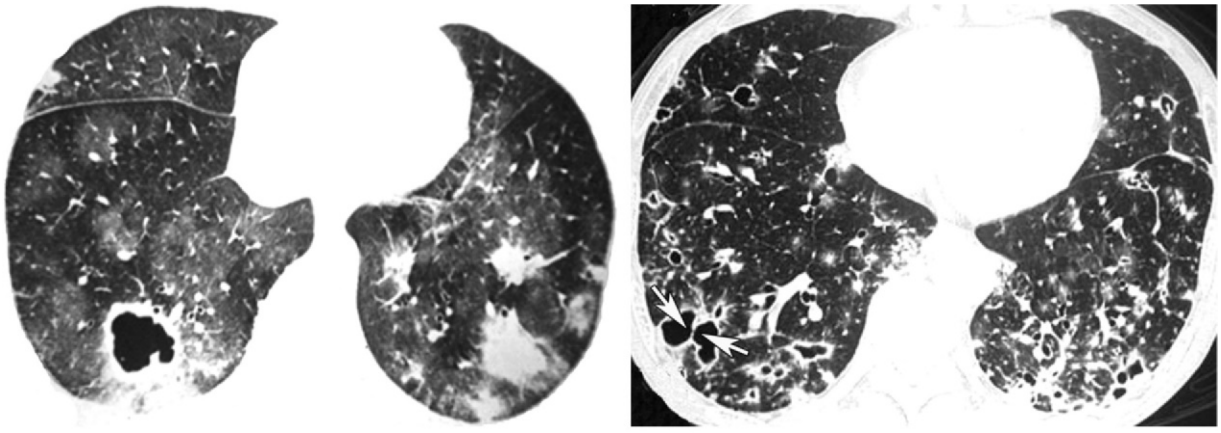

13. 14.

Figures 13, 14. **(13)** Chronic pulmonary PCM in a 48-year-old man. High-resolution CT scan shows large nodules with irregular borders in the left lower lobe, ground-glass attenuation, and a cavitated nodule with an irregular inner wall in the right lower lobe. **(14)** Chronic pulmonary PCM in a 40-year-old man. CT scan at the level of the lower lobes shows multiple thin-walled cystic lesions, small nodules, and bronchial wall thickening. A septated cyst can be seen in the posterior basal segment of the right lower lobe (arrows).

Cavitary Lesions

Consolidations, nodules, and masses tend to undergo necrosis and to cavitate, resulting in irregular-walled cavities (Fig 13). Cavitated nodules are common in untreated patients (17). These cavities may contain thickened interlobular septa, which remain intact, separating adjacent necrotic secondary pulmonary lobules (Fig 14) (10).

Halo Sign

The "halo" sign is nonspecific and may be seen in a wide spectrum of pulmonary diseases, although it is commonly associated with hemorrhagic nodules. Less frequently, the halo sign is associated with local pulmonary infiltration by inflammatory infiltrate, or with neoplasms such as adenocarcinoma (39,40). In the appropriate clinical setting, this sign may be the first evidence of invasive pulmonary fungal infection (41). To our knowledge, the halo sign has not been previously described in PCM (Fig 15).

Reversed Halo Sign

The "reversed halo" sign is a CT finding that consists of a focal round area of ground-glass attenuation surrounded by a relatively complete ring of consolidation (39). This sign was first described in the setting of cryptogenic organizing pneumonia but is not specific to this disease, since it was subsequently described in patients with PCM (16,39,42) and other infectious and noninfectious diseases (43–45).

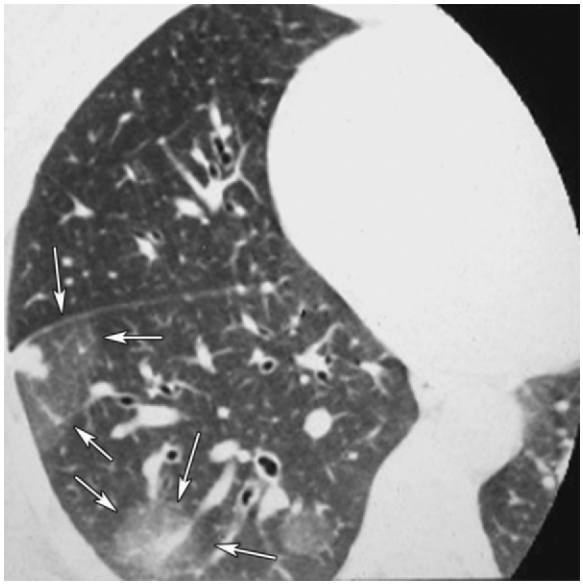

Figure 15. Chronic pulmonary PCM in a 47-year-old man. Close-up CT scan of the right lung depicts two pulmonary nodules (arrows) in the lower lobe, both of which are surrounded by areas of ground-glass attenuation (halo sign).

In PCM, the reversed halo sign is observed in approximately 10% of patients with active *P brasiliensis* infection. The halo can be single or multiple, ranging in size from 10 to 50 mm (average, 20 mm) (Fig 16). The distribution is predominantly in the middle and lower lung zones and in the lung periphery (16). Histologically, the central area of the lesions consists of an inflammatory infiltrate in the alveolar septa, with

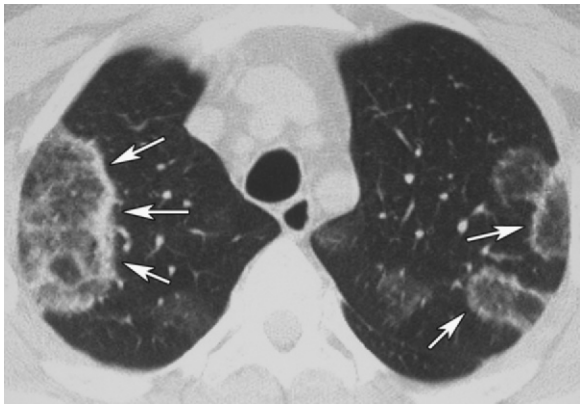

Figure 16. Chronic pulmonary PCM in a 57-year-old man. High-resolution CT scan at the level of the upper lobes demonstrates bilateral focal nodular ground-glass attenuation. Most of the nodules are surrounded by a ring of consolidation (reversed halo sign) (arrows).

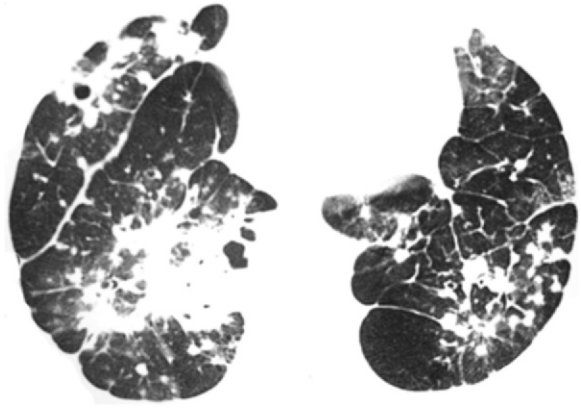

Figure 17. Chronic pulmonary PCM in a 69-year-old man. High-resolution CT scan at the level of the lower lobes shows interlobular septal thickening and multiple small nodules. Note the irregular cavitated lesion in the middle lobe and the nonhomogeneous areas of enhancement in the right lower lobe, associated with architectural distortion and bilateral paracicatricial emphysema.

relative preservation of the alveolar spaces. The periphery of the lesion consists of dense and homogeneous intraalveolar cellular infiltrate (16).

Interlobular Septal Thickening

Although interlobular septal thickening occurs in a significant number of cases, it rarely represents the predominant pattern (Fig 17). This finding is associated with the chronic form of infection and sequelae. The septal thickening pathologically corresponds to inflammatory infiltration or fibrosis (5,10).

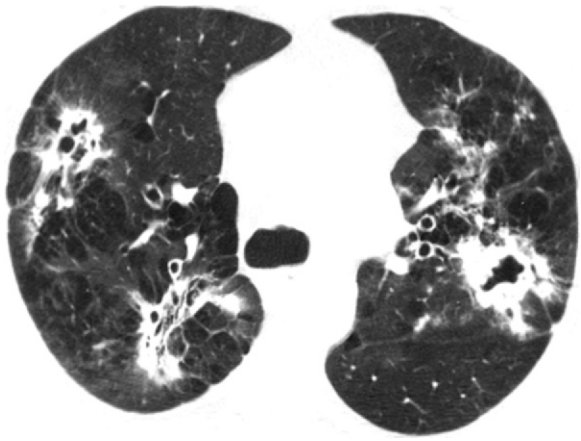

Figure 18. Chronic PCM in a 44-year-old man. High-resolution CT scan at the level of the carina shows irregular cavitated areas of enhancement associated with parenchymal distortion and paracicatricial emphysema.

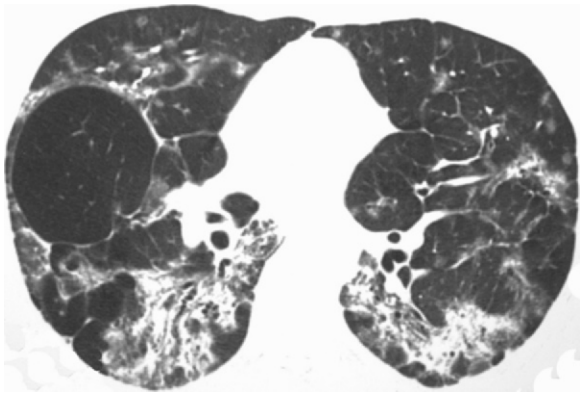

Figure 19. Chronic pulmonary PCM in a 63-year-old man. High-resolution CT scan shows emphysema associated with consolidations and ground-glass attenuation, traction bronchiectasis, and architectural distortion involving the lower lobes.

Fibrotic Pattern

Chronic evolution of PCM, along with the changes induced by treatment, leads to pulmonary fibrosis. The lung tissue, in addition to undergoing specific changes caused by the inflammatory process, is destroyed by progressive fibrosis (7). The fibrotic pattern consists of dense areas of fibrosis with prominent collagen deposition in perihilar regions. At CT, pulmonary fibrosis is characterized by peribronchovascular interstitial thickening, paracicatricial emphysema, traction bronchiectasis, parenchymal bands, and architectural distortion (Figs 18, 19) (5).

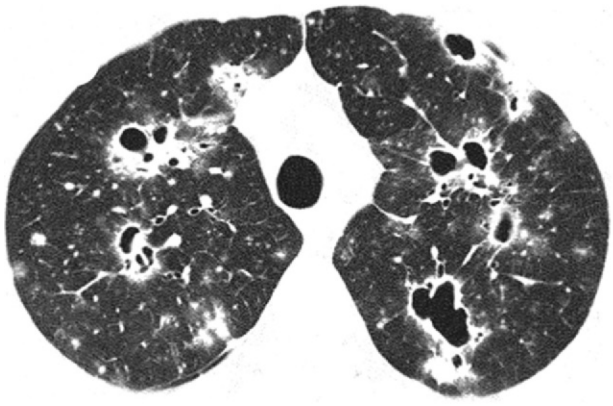

20a.

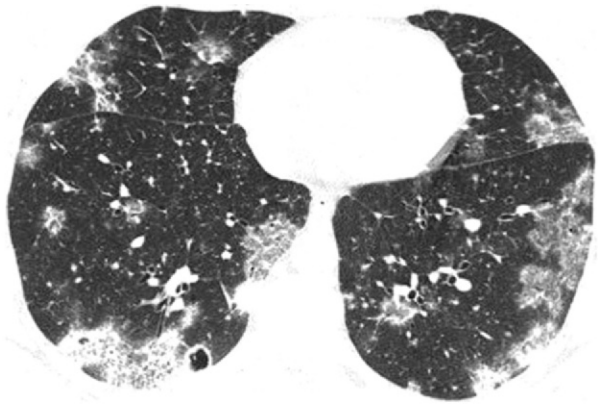

20b.

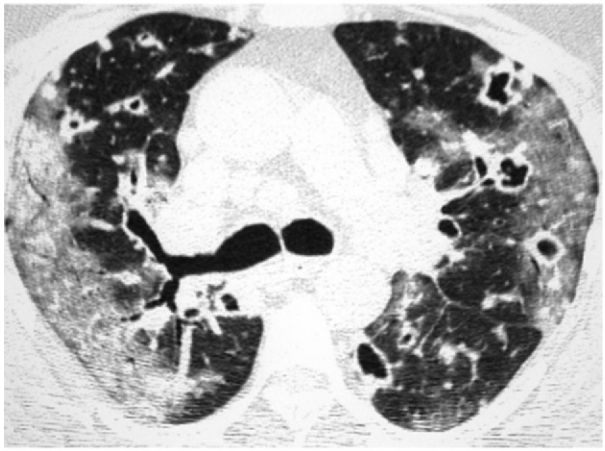

21.

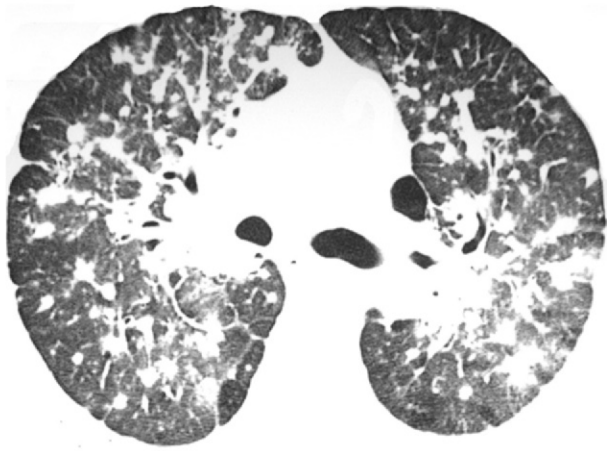

22.

Figures 20–22. **(20)** Chronic PCM in a 33-year-old man. **(a)** High-resolution CT scan at the level of the upper lobes shows cavitated lesions associated with several small nodules. **(b)** High-resolution CT scan shows multiple rounded areas of enhancement in a ground-glass pattern, mainly in the peripheral areas of the lower zones. **(21)** Chronic pulmonary PCM in a 29-year-old man. High-resolution CT scan at the level of the carina depicts areas of enhancement in a ground-glass pattern in the peripheral zones of both lungs, along with multiple cavitated nodules. **(22)** Chronic pulmonary PCM in a 43-year-old man with AIDS. High-resolution CT scan shows bilateral irregular nodules, diffuse ground-glass attenuation, and interlobular septal thickening, accompanied by mild architectural distortion.

Mixed Patterns

Patients with pulmonary PCM frequently present with a combination of features, including areas of ground-glass attenuation, variable-sized nodules, cavitary lesions, parenchymal bands, and areas of cicatricial emphysema (Figs 20, 21) (5,17,28). Signs of fibrosis are common in prolonged disease (7). Mixed patterns are also common in patients with AIDS (Fig 22).

Extrapulmonary Abnormalities

Although pulmonary findings are more common in the chronic form, PCM may manifest with extrapulmonary findings such as tracheal and lymph node involvement, pneumothorax, and osseous lesions.

Tracheal PCM and tuberculosis appear to disseminate in similar patterns. Dissemination may result from direct contact with infected sputum, extension of lymphatic drainage from parenchymal infection, or hematogenous spread (34). Granulomas and fibrosis are usually found around bronchi. CT of patients with tracheal PCM demonstrates irregular circumferential thickening of the tracheal wall, with submucosal nodules (Fig 23) (19). The differential diagnosis for diffuse wall thickening of the trachea at CT includes tuberculosis, sarcoidosis, amyloidosis, relapsing polychondritis, papillomatosis, rhinoscleroma, Wegener granulomatosis, and tracheopathia osteoplastica (46).

Although PCM involves the lymphatic system, enlarged mediastinal or hilar lymph nodes are uncommon. Lymphadenopathy has been

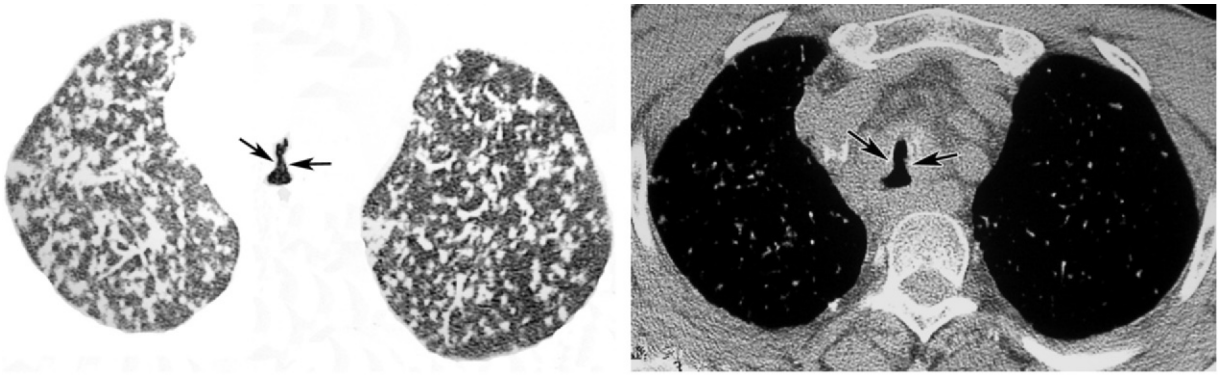

a. b.

Figure 23. Chronic pulmonary PCM in a 46-year-old man. CT scans obtained with lung **(a)** and mediastinal **(b)** windows reveal circumferential thickening of the tracheal wall with irregular luminal narrowing (arrows). Both lungs also exhibit irregular micronodules in a random distribution.

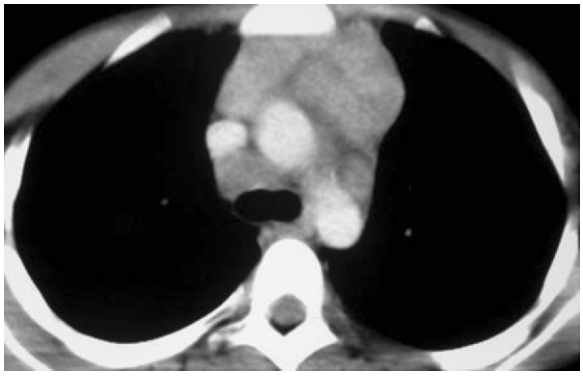

Figure 24. Acute PCM in a 17-year-old boy. Contrast material–enhanced CT scan (mediastinal window) demonstrates enlarged prevascular, paraaortic, and lower paratracheal nodes. The pulmonary parenchyma was normal.

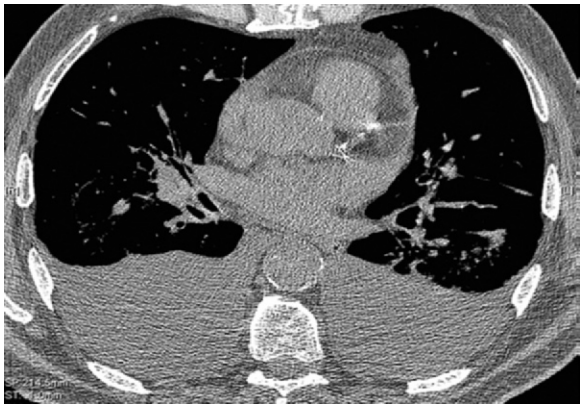

Figure 25. Acute disseminated PCM in a 27-year-old man. CT scan (mediastinal window) shows bilateral pleural effusion.

reported in only 13% of cases (Fig 24), and pleural effusion is uncommon in both the acute (Fig 25) and chronic forms, although a few cases have been reported (5,17,27,47). In their study

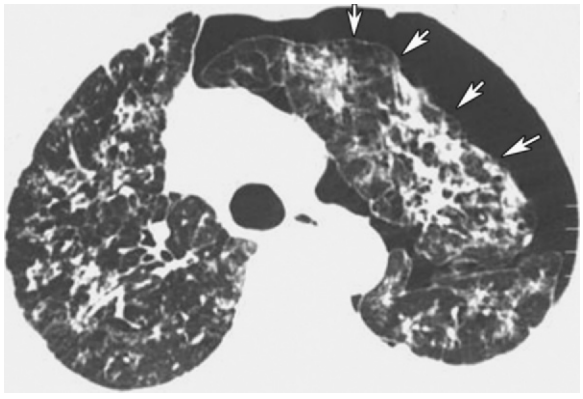

Figure 26. Chronic pulmonary PCM in a 45-year-old man. High-resolution CT scan at the level of the upper lobes demonstrates multiple irregular nodules in both lungs, with signs of architectural distortion, interlobular septal thickening, and emphysema, in addition to left pneumothorax (arrows).

of 153 chest radiographs obtained in patients with PCM, do Valle et al (18) reported four cases of pleural effusion (unilateral in three cases and bilateral in one case). A case of pneumothorax secondary to PCM has been reported (Fig 26), probably caused by rupture of an air-containing space (emphysema with or without bulla formation, or a cavitated lesion) (48).

Bone involvement in PCM is uncommon and results primarily from hematogenous dissemination. A radiologic review of 173 consecutive cases of acute and chronic PCM showed bone lesions in only 1.7% of cases (15). Another study of high-resolution CT scans obtained in 77 patients with chronic PCM found no bone involvement (17). Although rare, bone and joint lesions occur more frequently in the juvenile (acute) form of PCM, particularly in children (26). For this

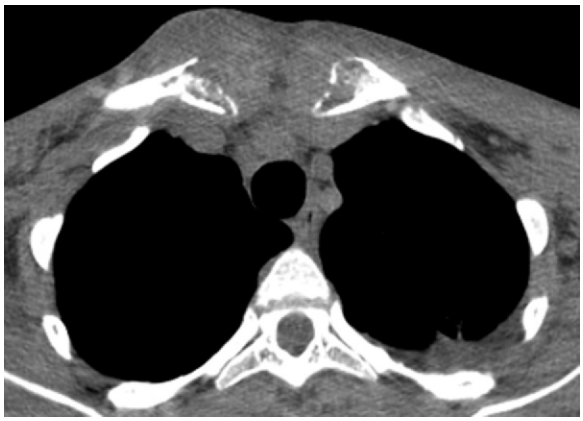

Figure 27. Acute disseminated PCM in a 24-year-old man. CT scan demonstrates involvement of the anterior chest wall by clavicular osteolytic lesions and a soft-tissue mass.

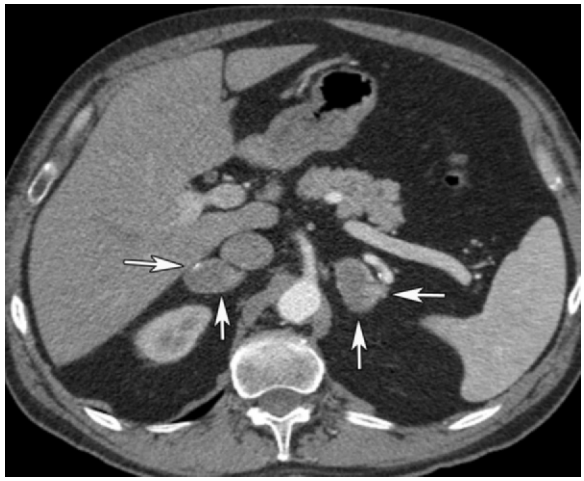

Figure 28. Chronic PCM in a 57-year-old man. CT scan of the superior abdomen shows bilateral adrenal masses (arrows).

reason, the association of pulmonary and bone lesions is extremely rare. In a study by Marchior (49), pulmonary lesions were present in only one of 20 patients (5%) with proved PCM bone lesions.

Osseous involvement can occur in any skeletal bone; however, these lesions are more common in the chest, shoulder girdle, and long bones (22,49,50). Osteolytic lesions usually have indistinct margins (Fig 27) and cannot be radiologically distinguished from other forms of osteomyelitis. The differential diagnosis includes other fungal diseases, chronic bacterial osteomyelitis, tuberculosis, and malignancies such as lymphoma and metastasis (51). In endemic areas, PCM must be considered in the differential diagnosis of bone lesions in AIDS patients (50). In addition, once the upper abdominal organs are (at least in part) routinely seen on chest CT scans, involvement of the liver, spleen, or adrenal glands may be observed (Fig 28).

Conclusions

PCM is the most common systemic mycosis in Latin America and is particularly prevalent in Brazil. Because of increased travel to and emigration from endemic areas, several cases of PCM have been reported in Europe and North America. Chronic PCM is the most common form of the disease and frequently manifests with pulmonary involvement. To avoid the progression of mycosis and irreversible lung damage in patients with pulmonary CT features of PCM, the diagnosis should be reached rapidly and therapy for the infection should be initiated. If left untreated, systemic PCM can be severe and fatal. PCM is rarely suspected in nonendemic areas because of the extremely lengthy silent period of the disease (17,22,52).

Pulmonary PCM has a variety of radiologic manifestations, including airspace consolidations, focal masses, nodules, miliary disease, interstitial disease, and cavitary lesions. Fibrosis and paracicatricial emphysema are common associated findings, and mixed patterns are frequently seen in a single patient. Extrapulmonary findings in the thorax are uncommon but include tracheal, pleural, and lymph node involvement, as well as osseous lesions. The diagnosis is often delayed because pulmonary PCM can mimic many other conditions, including bacterial pneumonia, other fungal diseases, malignancy, and tuberculosis. Although PCM infection often manifests with nonspecific abnormalities, awareness of its multiple radiologic manifestations as well as its epidemiologic and clinical characteristics may permit early diagnosis and reduce associated morbidity and mortality.

References

1. Ferreira MS. Paracoccidioidomycosis. Paediatr Respir Rev 2009;10(4):161–165.
2. Benoldi D, Alinovi A, Pezzarossa E, Bassissi P, Polonelli L. Paracoccidioidomycosis (South American blastomycosis): a report of an imported case previously diagnosed as tuberculosis. Eur J Epidemiol 1985;1(2):150–152.

3. Mayayo E, López-Aracil V, Fernández-Torres B, Mayayo R, Domínguez M. Report of an imported cutaneous disseminated case of paracoccidioidomycosis. Rev Iberoam Micol 2007;24(1):44–46.
4. Benard G, Kavakama J, Mendes-Giannini MJ, Kono A, Duarte AJ, Shikanai-Yasuda MA. Contribution to the natural history of paracoccidioidomycosis: identification of the primary pulmonary infection in the severe acute form of the disease—a case report. Clin Infect Dis 2005;40(1):e1–e4.
5. Funari M, Kavakama J, Shikanai-Yasuda MA, et al. Chronic pulmonary paracoccidioidomycosis (South American blastomycosis): high-resolution CT findings in 41 patients. AJR Am J Roentgenol 1999;173(1):59–64.
6. dos Santos JW, Severo LC, Porto NdaS, Moreira JdaS, da Silva LC, Carmargo JJ. Chronic pulmonary paracoccidioidomycosis in the state of Rio Grande do Sul, Brazil. Mycopathologia 1999;145(2):63–67.
7. Tobón AM, Agudelo CA, Osório ML, et al. Residual pulmonary abnormalities in adult patients with chronic paracoccidioidomycosis: prolonged follow-up after itraconazole therapy. Clin Infect Dis 2003;37(7):898–904.
8. Goldani LZ, Sugar AM. Paracoccidioidomycosis and AIDS: an overview. Clin Infect Dis 1995;21(5):1275–1281.
9. Borges-Walmsley MI, Chen D, Shu X, Walmsley AR. The pathobiology of Paracoccidioides brasiliensis. Trends Microbiol 2002;10(2):80–87.
10. Marchiori E, Valiante PM, Mano CM, et al. Paracoccidioidomycosis: high-resolution computed tomography–pathologic correlation. Eur J Radiol 2011;77(1):80–84.
11. Blotta MH, Mamoni RL, Oliveira SJ, et al. Endemic regions of paracoccidioidomycosis in Brazil: a clinical and epidemiologic study of 584 cases in the southeast region. Am J Trop Med Hyg 1999;61(3):390–394.
12. Brummer E, Castaneda E, Restrepo A. Paracoccidioidomycosis: an update. Clin Microbiol Rev 1993;6(2):89–117.
13. Coutinho ZF, Silva D, Lazera M, et al. Paracoccidioidomycosis mortality in Brazil (1980–1995). Cad Saude Publica 2002;18(5):1441–1454.
14. Gasparetto EL, Liu CB, de Carvalho Neto A, Rogacheski E. Central nervous system paracoccidioidomycosis: imaging findings in 17 cases. J Comput Assist Tomogr 2003;27(1):12–17.
15. Trad HS, Trad CS, Elias J Jr, Muglia VF. Radiological review of 173 consecutive cases of paracoccidioidomycosis [in Portuguese]. Radiol Bras 2006;39(3):175–179.
16. Gasparetto EL, Escuissato DL, Davaus T, et al. Reversed halo sign in pulmonary paracoccidioidomycosis. AJR Am J Roentgenol 2005;184(6):1932–1934.
17. Souza AS Jr, Gasparetto EL, Davaus T, Escuissato DL, Marchiori E. High-resolution CT findings of 77 patients with untreated pulmonary paracoccidioidomycosis. AJR Am J Roentgenol 2006;187(5):1248–1252.
18. do Valle AC, Guimarães RR, Lopes DJ, Capone D. Thoracic radiologic aspects in paracoccidioidomycosis [in Portuguese]. Rev Inst Med Trop Sao Paulo 1992;34(2):107–115.
19. Marchiori E, Escuissato DL, Souza AS Jr, Barillo JL, Warszawiak D, de Souza AS. Computed tomography findings in patients with tracheal paracoccidioidomycosis. J Comput Assist Tomogr 2008;32(5):788–791.
20. Bethlem EP, Capone D, Maranhão B, Carvalho CRR, Wanke B. Paracoccidioidomycosis. Curr Opin Pulm Med 1999;5(5):319–325.
21. Ramos-E-Silva M, Saraiva LdoE. Paracoccidioidomycosis. Dermatol Clin 2008;26(2):257–269, vii.
22. Ameen M, Talhari C, Talhari S. Advances in paracoccidioidomycosis. Clin Exp Dermatol 2010;35(6):576–580.
23. Rivitti EA, Aoki V. Deep fungal infections in tropical countries. Clin Dermatol 1999;17(2):171–190; discussion 105–106.
24. Muniz MA, Marchiori E, Magnago M, Moreira LB, de Almeida JG Jr. High-resolution computed tomography findings in pulmonary paracoccidioidomycosis [in Portuguese]. Radiol Bras 2002;35(3):147–154.
25. Nogueira SA, Guedes AL, Wanke B, et al. Osteomyelitis caused by Paracoccidioides brasiliensis in a child from the metropolitan area of Rio de Janeiro. J Trop Pediatr 2001;47(5):311–315.
26. Nogueira MG, Andrade GM, Tonelli E. Clinical evolution of paracoccidioidomycosis in 38 children and teenagers. Mycopathologia 2006;161(2):73–81.
27. Pellegrino A, de Capriles CH, Magaldi S, et al. Severe juvenile type paracoccidioidomycosis with hepatitis C. Am J Trop Med Hyg 2003;68(3):301–303.
28. dos Santos JW, Debiasi RB, Miletho JN, Bertolazi AN, Fagundes AL, Michel GT. Asymptomatic presentation of chronic pulmonary paracoccidioidomycosis: case report and review. Mycopathologia 2004;157(1):53–57.
29. Achenbach R, Negroni R, Khaski S, Lococo L, Beresñak A, Gai L. Paracoccidioidomycosis: unusual clinical presentation and utility of computerized tomography scanning for diagnosis. Int J Dermatol 2002;41(12):881–882.
30. Paniago AM, Aguiar JI, Aguiar ES, et al. Paracoccidioidomycosis: a clinical and epidemiological study of 422 cases observed in Mato Grosso do Sul [in Portuguese]. Rev Soc Bras Med Trop 2003;36(4):455–459.
31. García Bustínduy M, Guimerá FJ, Arévalo P, et al. Cutaneous primary paracoccidioidomycosis. J Eur Acad Dermatol Venereol 2000;14(2):113–117.
32. Marchiori E, Gasparetto EL, Escuissato DL, Souza AS Jr, Barreto MM. Pulmonary paracoccidioidomycosis and AIDS: high-resolution CT findings in five patients. J Comput Assist Tomogr 2007;31(4):605–607.

33. Benard G, Duarte AJ. Paracoccidioidomycosis: a model for evaluation of the effects of human immunodeficiency virus infection on the natural history of endemic tropical diseases. Clin Infect Dis 2000; 31(4):1032–1039.
34. Tuder RM, el Ibrahim R, Godoy CE, De Brito T. Pathology of the human pulmonary paracoccidioidomycosis. Mycopathologia 1985;92(3):179–188.
35. Franco MF, Montenegro MR. Anatomia patológica. In: Del Negro G, Lacaz SF, Fiorillo DM, eds. Paracoccidioidomycosis. São Paulo, Brazil: Sarvier/Edusp, 1982.
36. Cunha Motta L. Paracoccidiodal granuloma (Blastomycosis brasiliensis) [in Portuguese]. An Fac Med Univ S Paulo 1942;18:145–159.
37. Ortega AA, Pollak L. Paracoccidioidomycosis. In: Baker RD, ed. The pathologic anatomy of mycoses. Berlin, Germany: Springer-Verlag, 1971.
38. Freitas RM, Prado R, Prado FL, et al. Pulmonary paracoccidioidomycosis: radiology and clinical-epidemiological evaluation. Rev Soc Bras Med Trop 2010;43(6):651–656.
39. Hansell DM, Bankier AA, MacMahon H, McLoud TC, Müller NL, Remy J. Fleischner Society: glossary of terms for thoracic imaging. Radiology 2008;246(3):697–722.
40. Primack SL, Hartman TE, Lee KS, Müller NL. Pulmonary nodules and the CT halo sign. Radiology 1994;190(2):513–515.
41. Pinto PS. The CT halo sign. Radiology 2004;230 (1):109–110.
42. Kim SJ, Lee KS, Ryu YH, et al. Reversed halo sign on high-resolution CT of cryptogenic organizing pneumonia: diagnostic implications. AJR Am J Roentgenol 2003;180(5):1251–1254.
43. Marchiori E, Grando RD, Simões Dos Santos CE, et al. Pulmonary tuberculosis associated with the reversed halo sign on high-resolution CT. Br J Radiol 2010;83(987):e58–e60.
44. Marchiori E, Zanetti G, Hochhegger B, Irion KL. Re: reversed halo sign: nodular wall as criterion for differentiation between cryptogenic organizing pneumonia and active granulomatous diseases. Clin Radiol 2010;65(9):770–771.
45. Wahba H, Truong MT, Lei X, Kontoyiannis DP, Marom EM. Reversed halo sign in invasive pulmonary fungal infections. Clin Infect Dis 2008;46(11):1733–1737.
46. Prince JS, Duhamel DR, Levin DL, Harrell JH, Friedman PJ. Nonneoplastic lesions of the tracheobronchial wall: radiologic findings with bronchoscopic correlation. RadioGraphics 2002; 22(spec no): S215–S230.
47. Slevogt H, Tintelnot K, Seybold J, Suttorp N. Lymphadenopathy in a pregnant woman from Brazil. Lancet 2004;363(9417):1282.
48. Pereira ML, Marchiori E, Zanetti G, et al. Spontaneous pneumothorax as an atypical presentation of pulmonary paracoccidioidomycosis: a case report with emphasis on the imaging findings. Case Report Med 2010;2010:961984.
49. Marchiori E. Bone and joints radiological findings in paracoccidioidomycosis [in Portuguese]. Radiol Bras 1989;22(1):5–16.
50. de Freitas RS, Dantas KC, Garcia RS, Magri MM, de Andrade HF Jr. Paracoccidioides brasiliensis causing a rib lesion in an adult AIDS patient. Hum Pathol 2010;41(9):1350–1354.
51. Valera ET, Mori BM, Engel EE, et al. Fungal infection by Paracoccidioides brasiliensis mimicking bone tumor. Pediatr Blood Cancer 2008;50(6):1284–1286.
52. Buitrago MJ, Bernal-Martínez L, Castelli MV, Rodríguez-Tudela JL, Cuenca-Estrella M. Histoplasmosis and paracoccidioidomycosis in a non-endemic area: a review of cases and diagnosis. J Travel Med 2011;18(1):26–33.

Thoracic Paracoccidioidomycosis: Radiographic and CT Findings

Miriam M. Barreto, MD, PhD • Edson Marchiori, MD, PhD • Viviane B. Amorim, MD • Gláucia Zanetti, MD • Tatiana C. Takayassu, MD • Dante L. Escuissato, MD, PhD • Arthur S. Souza, Jr, MD, PhD • Rosana S. • Rodrigues, MD, PhD

RadioGraphics 2012; 32:71–84 • **Published online** 10.1148/rg.321115052 • **Content Codes:** CH CT

Page 72
The lungs are the main target organ of *P brasiliensis*, and chronic changes are responsible for the morbidity and mortality associated with PCM (5). Active pulmonary involvement has been reported in 80% of PCM cases and residual fibrotic lesions in 60% (7).

Page 72
The diagnosis of PCM is established with visualization of *P brasiliensis*, either at direct examination or after isolation of the fungus at culture, in biologic specimens such as sputum, bronchoalveolar lavage fluid, smears from mucocutaneous lesions, or tissue biopsy samples from laryngeal lesions, cervical lymph nodes, or lung (10).

Page 73
Clinical forms of PCM range from a benign self-limited infection to a severe, progressive, and sometimes fatal disease involving pulmonary and extrapulmonary tissues. The two main clinical forms of PCM are the acute form (juvenile type) and the chronic form (adult type). The chronic form of the disease may develop many years after patients have left an endemic area (3,4,11,12,25,26).

Page 75
Chest radiographic lung abnormalities in chronic PCM are frequently multiple and nonspecific (7,38). They have been variously described as linear reticular opacities, nodules of various sizes, patchy ill-defined opacities, airspace consolidation, and cavitation (5,6,10,15,17,18,38).

Page 75
The most common CT findings of chronic PCM are ground-glass areas of enhancement, consolidations, variable-sized nodules, masses, cavitations, interlobular septal thickening, and fibrotic lesions (5,17). A combination of these findings is observed in most cases and may be focal, multifocal, or diffuse.